

Article

Reversible Bonding of Thermoplastic Elastomers for Cell Patterning Applications

Byeong-Ui Moon *, Keith Morton, Kebin Li, Caroline Miville-Godin and Teodor Veres *

Life Sciences Division, National Research Council of Canada, 75, de Mortagne Blvd.,
Boucherville, QC J4B 6Y4, Canada; Keith.Morton@cnrc-nrc.gc.ca (K.M.); Kebin.Li@cnrc-nrc.gc.ca (K.L.);
Caroline.Miville-Godin@cnrc-nrc.gc.ca (C.M.-G.)

* Correspondence: Ben.Moon@cnrc-nrc.gc.ca (B.-U.M.); Teodor.Verres@cnrc-nrc.gc.ca (T.V.)

Abstract: In this paper, we present a simple, versatile method that creates patterns for cell migration studies using thermoplastic elastomer (TPE). The TPE material used here can be robustly, but reversibly, bonded to a variety of plastic substrates, allowing patterning of cultured cells in a microenvironment. We first examine the bonding strength of TPE to glass and polystyrene substrates and compare it to thermoset silicone-based PDMS under various conditions and demonstrate that the TPE can be strongly and reversibly bonded on commercially available polystyrene culture plates. In cell migration studies, cell patterns are templated around TPE features cored from a thin TPE film. We show that the significance of fibroblast cell growth with fetal bovine serum (FBS)-cell culture media compared to the cells cultured without FBS, analyzed over two days of cell culture. This simple approach allows us to generate cell patterns without harsh manipulations like scratch assays and to avoid damaging the cells. We also confirm that the TPE material is non-toxic to cell growth and supports a high viability of fibroblasts and breast cancer cells. We anticipate this TPE-based patterning approach can be further utilized for many other cell patterning applications such as in cell-to-cell communication studies.

Keywords: thermoplastic elastomers; cell patterning; cell migration; reversible bonding



Citation: Moon, B.-U.; Morton, K.; Li, K.; Miville-Godin, C.; Veres, T. Reversible Bonding of Thermoplastic Elastomers for Cell Patterning Applications. *Processes* **2021**, *9*, 54. <https://doi.org/10.3390/pr9010054>

Received: 8 December 2020

Accepted: 24 December 2020

Published: 29 December 2020

Publisher's Note: MDPI stays neutral with regard to jurisdictional claims in published maps and institutional affiliations.



Copyright: © 2020 by the authors. Licensee MDPI, Basel, Switzerland. This article is an open access article distributed under the terms and conditions of the Creative Commons Attribution (CC BY) license (<https://creativecommons.org/licenses/by/4.0/>).

1. Introduction

Cell patterning provides a simple and low-cost method for cell migration studies. Many technologies have been developed to pattern cells within in vitro microenvironments to enable the study of cell migration including invasion into transwell inserts, Boyden chamber assays [1], scratch assays [2], ring barrier assays [3], and aqueous two-phase cell patterning [4]. Although these approaches use basic 2D cell culture platforms, they offer a wide variety of possible cell assay applications. Recently, microfluidic-based models have emerged as powerful platforms to study cell migration and/or angiogenesis [5]. The chip-based models enable formation of 3D architecture blood vessels and the study of soluble biochemistry in discrete fluidic channel networks [6], as well as the study of epithelial-endothelial migration in breast cancer [7]. These novel microfluidic approaches closely mimic both physiological and pathological microenvironments and there is a significant effort to apply these technologies to new drug screening and therapeutic applications. However, microfluidic device fabrication usually involves complicated cleanroom facilities and requires highly sophisticated processes which are costly and labor-intensive [6–9]. Moreover, poly(dimethylsiloxane) (PDMS) is a commonly used material in the prototype of microfluidic devices. However its intrinsic physical and chemical properties such as porous polymer network, native hydrophobic surface and fast hydrophobic recovery after hydrophilic surface treatment can result in significant adsorption and absorption of hydrophobic drugs and their metabolites, limiting the utility of PDMS in biomedical microfluidic applications [10,11]. Therefore, it is greatly preferable to take thermoplastic

(TP)-based substrates and devices, for which cell behavior and functions have already been proven that over many decades in the biology community [12].

TP materials are well-known cell culture substrates. Due to their high biocompatibility, low-cytotoxicity, minimal drugs absorption and high optical transparency, they have been used extensively in 3D cell culture platforms [7,13], as biocompatible substrates for cellular contact guidance [14], lab-on-a-chip devices [15], and other biomedical applications generally [16]. A subset class of TP materials called thermoplastic elastomers (TPEs) are also soft and flexible offering distinct advantages in manufacturing processes. These TPE based devices can be fabricated by using hot-embossing, thermoforming or injection molding in a high-throughput and scalable manner, an increasingly attractive prospect to the researchers in the microfluidic community. Compared to solid TP polymers, TPEs can attach conformably to other TP materials and provide a robust seal due to their inherent compliance. A reversibly bonding process is typically straightforward between TPE and other TPs, while TP/TP assembly methods typically require high temperatures and pressures for thermal fusion bonding [17–19], additional structures in solvent bonding [20], and the introduction of UV-curable resins for adhesive bonding [21], to fully assemble microfluidic devices. In contrast, TPE bonding can be achieved at mild temperatures (room temperature to ~ 80 °C) and is possible without any pretreatment in the case of reversible bonded devices.

For many microfluidic devices, device assembly often requires permanent bonding in order to avoid delamination or fluid leaks. However, a reversible bonding has some advantages in modern biomedical applications, such as microfluidic patterning of miniaturizing DNA arrays [22], and cell culture systems where subsequent cell harvesting is required. To manage cell or tissue sample collections, it is highly desirable to have easy access to the fluidic channels and cell chambers after microfluidic processing [23]. Self-adhesion (reversible) bonding is a well-known method in PDMS device construction. When a PDMS device is simply placed on a flat substrate, it forms weak Van der Waal's bonds with certain hydroxyl groups present on materials such as itself, glass and silicon. However, the self-adhesion strength of PDMS bonding is very weak and it can only provide leak-free flow when the applied pressure is below 35 kPa [24,25]. Alternatively, TPE materials offer a stronger fluid tight seal than PDMS with improved bonding in microfluidic devices [26,27].

Here we describe a new technique that creates patterns using TPE thin films for cell migration studies. The cell patterns are templated around a TPE feature made from a flattened TPE film using a biopsy punch. We first examine the bonding strength of TPE on a variety of substrates and directly compare bonding strength to PDMS equivalents under similar conditions. Next, for cell migration studies, we prepared TPE posts and positioned them in individual well of 96-well plates prior to first seeding of fibroblast cells in the wells. After the TPE post removal, we examine and analyze cell migration over 2 days in two different culture media conditions. Lastly, we also evaluate cell cytotoxicity of the TPE material with fibroblasts and breast cancer cells.

For the first time, we show a wholly plastic-based approach to generate cell patterning without more complicated photolithography-based processes and demonstrate its capability for cell migration study.

2. Experimental Section

2.1. TPE Bonding test Devices and Post Preparation

Mediprene OF 400M were received from Hexpol TPE (HEXPOL AB, Malmö, Sweden) in the form of pellets. The pellets are extruded at 165 °C to form thin films (between 0.2 mm and 4 mm thick and several 10 s of meters in length). Here we used 3-mm-thick TPE sheets flattened after extrusion by hot-embossing using flat, silanized silicon wafers as unstructured mold to make flat, smooth, films. Hot-embossing was performed under nominal vacuum using an EVG 520 system (EV Group, Sankt Florian am Inn, Austria) at a temperature of 125 °C, an applied force of 10 kN.

The TPE posts were prepared with a biopsy punch (ThermoFisher, Waltham, MA, USA). Figure 1 shows images of the prepared TPE posts. We used a 1 mm diameter biopsy punch with core plunger to make and eject the TPE posts (Figure 1a). After punching through the processed TPE films, the TPE posts were collected using a tweezer. Cleaning of the posts was followed by immersion in 70% ethanol (1 h), phosphate-buffered saline (PBS) (1 h) followed by drying in an N₂ stream. For the subsequent cell culture experiments, the TPE posts are attached on the 96-well plate (Figure 1b,c).

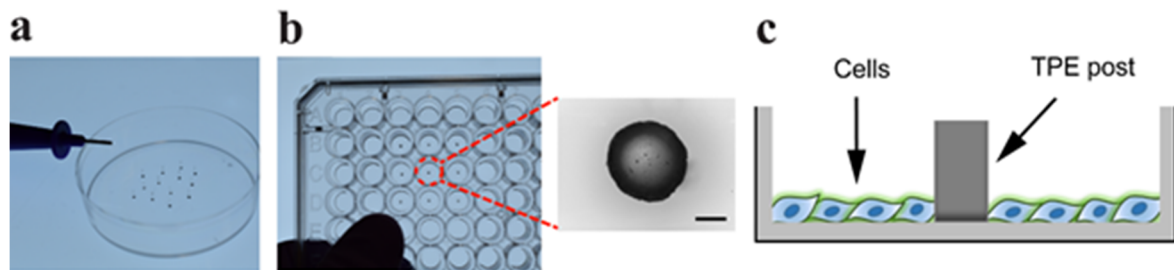


Figure 1. Thermoplastic elastomer (TPE) post preparation: (a) TPE posts were made using a 1 mm diameter biopsy punch (b) and attached in center of individual wells of a 96-well cell culture plate. The image inset shows the rounded shape of the TPE post. The scale bar represents 200 μm . (c) Schematic drawing of the TPE-assisted cell patterning platform.

In order to perform the TPE bonding strength experiments, we prepared a simple microfluidic device consisting of three chambers (0.8 mm diameter) each connected by a single, 100 μm width microfluidic channel. An array of 10 μm diameter micropillars (Figure 2a) are monolithically integrated in the chamber to avoid chamber collapse. We prepared both TPE and PDMS-casted devices for a comparison study. For the TPE devices, a fluorinated ethylene propylene (FEP, McMaster-Carr, Robbinsville, NJ, USA) mold was first replicated from a Si master mold which was fabricated by standard photo-lithography (EVG6200, EV Group, Sankt Florian am Inn, Austria) and a deep reactive ion etching process (Plasmalab100, Oxford Instruments, Abingdon, UK) on Si wafer. The replica FEP mold is then used to make TPE devices by hot-embossing. Details about the mold fabrication and hot-embossing conditions could be found in our previous work [28,29]. For the PDMS devices, standard soft-lithography techniques were used. A volume ratio of 10:1 (base to curing agent) of PDMS (Sylgard 184, Dow Corning Co., Midland, MI, USA) was cast on the same FEP mold and cured in the oven at 80 $^{\circ}\text{C}$ for 4 h.

The device was assembled by the following way. Entrance holes in diameter of 1.2 mm were first punched by a commercial puncher (Harris Uni-Core™, ThermoFisher, Waltham, MA, USA). After cleaning with IPA or methanol and drying by N₂ blowing. The two slabs of TPE and glass or PS substrates were then brought together without any external force and surface treatment. After this bonding process, a luer connector was placed on top of the device by aligning with the entrance hole on the device (Figure 2a). The bonding strength of TPE on glass and PS substrates is referred to as “delamination pressure” and was measured on the test platform following three thermal treatment conditions: (i) room temperature (RT) assembly, (ii) heat treatment at 37 $^{\circ}\text{C}$ for 2 h, and (iii) heat treatment at 65 $^{\circ}\text{C}$ for 2 h after assembly.

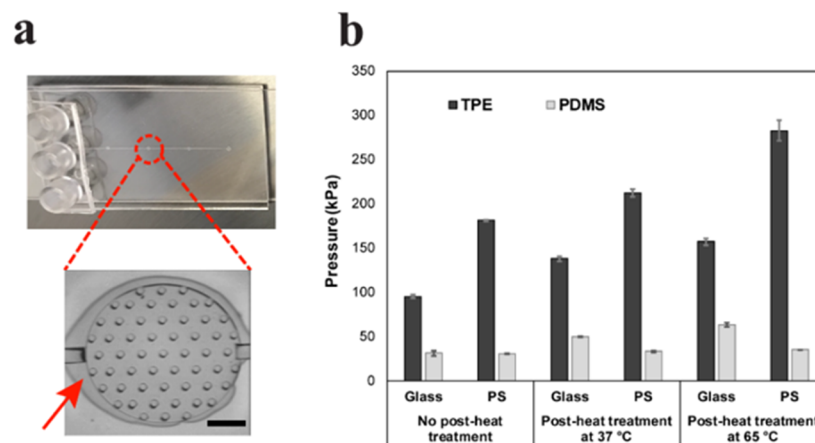


Figure 2. TPE Bonding test device and delamination pressure under different conditions. (a) A photograph of an assembled device for delamination testing. The zoomed-in image shows in the area of an array of micropillars. A representative microscopy image shows a fully delaminated TPE chamber on the glass slide as the applied pressure is increased. A red arrow bar indicates a delaminated area. The scale bar represents 200 μm . (b) A comparison bar graph of bonding strengths for TPE and PDMS on both glass slides and PS substrates under three different thermal treatment conditions (with standard errors calculated from the data measured on four samples).

The pneumatic pressure testing platform consisted of an instrumented pneumatic manifold, designed and built in-house, with 16 independent pressure regulation channels driven by 32 three-way electromagnetic valves (LHDA2423111H, The Lee Company, Westbrook, CT, USA). Valve opening and closing operations were controlled through a custom Labview GUI interface (National Instruments, Austin, TX, USA) [28,30]. The delamination of the TPE or PDMS material from the substrates were monitored and recorded using an inverted microscope (Eclipse TE-2000-U, Nikon, Tokyo, Japan). The delamination usually starts from the individual small micropillars and then propagates to the edge of the chamber with increasing applied pressure to the chamber through the 100 μm wide channel. The bonding strength is defined as the pressure starting to delaminate from the substrate to the edge of the chamber as shown in Figure 2a, a red arrow bar.

2.2. Cell Culture

Primary neonatal normal human dermal fibroblasts (NHDFs) and breast cancer cell (MCF-7) were purchased from ATCC (Manassas, VA, USA). Cells were thawed and cultured in Dulbecco's Modified Eagle Medium (DMEM), 10% fetal bovine serum (FBS), penicillin (100 units/mL), and streptomycin (100 $\mu\text{g}/\text{mL}$) in T-25 culture flasks at 37 $^{\circ}\text{C}$ incubator with 5% CO_2 (passage numbers of NHDF P3-P6 and MCF-7 P10-P15). After TPE posts attachment on the 96-well plate, we seeded the cells at the density of 10,000 cells per well and continued to let the cells culture. The TPE posts were then removed manually two days following cell seeding. Upon the TPE removal, cells continued to be cultured in DMEM with and without FBS by exchanging media every day.

2.3. Immunocytochemistry

For the assessment of cell migration assay, cells were labeled on day 1 with CellTracker Red (Cat. #C34552, ThermoFisher, Waltham, MA, USA). A 10 μM CellTracker Red working solution was prepared in an Opti-MEM (Cat. #31985070, ThermoFisher, Waltham, MA, USA) media and introduced in the well plate. The cells were then incubated at 37 $^{\circ}\text{C}$ in the CO_2 incubator for 30 min after which fresh media is exchanged and cell images are taken for further analysis. For the quantification of fibroblast migration assay, cell were fixed with 4% formaldehyde and followed by the treatment with 0.2% Triton X-100 for permeabilization. After washing with PBS, Fluorescein isothiocyanate(FITC)-

conjugated phalloidin (P5282, Sigma-Aldrich, St. Louis, MO, USA) and Hoechst 33342 (Cat. # H3570, ThermoFisher, Waltham, MA, USA) were diluted in a PBS blocking buffer (Cat. #37515, ThermoFisher) with 1:100 and 1:500 dilution ratios, respectively. The 96-well plate containing the mixture was then incubated at room temperature for 1 h. Stained cell images are obtained by fluorescence microscopy (EVOS FL, ThermoFisher) using 10× and 4× objectives.

2.4. Live/Dead Cell Imaging

The effect of TPE on cell viability was tested by preparing TPE plugs and the commercially available imaging kit. An injection molded TPE material was cut into a plug type that can be mounted on the top of the 96-well plate. These TPE plugs were then sterilized in 70% ethanol and D.I. water. The plugs were submerged into cell culture media after cell seeding. We examined two different cell types of neonatal normal human dermal fibroblasts (NHDF) and a breast cancer cell line (MCF-7). The cells were seeded on the 96-well plate (10k cell per well) and cultured in Dulbecco's Modified Eagle Medium (DMEM), containing 10% FBS, penicillin (100 units/mL), and streptomycin (100 µg/mL). We added 320 µL culture media in each well and cultured in an incubator at 37 °C and 5% CO₂ for 72 h. We performed cell cytotoxicity experiments for the TPE material using LIVE/DEAD Cell Imaging Kit (ThermoFisher, Waltham, MA, USA). For the cell imaging process, we added a mixture of live/dead solutions and let the cells incubate for 20 min at room temperature. The stained cells were imaged with an inverted fluorescence microscope (EVOS FL, ThermoFisher) using 4× and 10× objectives. The captured images were post-processed using ImageJ Software (NIH, Bethesda, MD, USA) to assess cell viability using the ratio between the numbers of living cells to the total number of cells.

2.5. Image Analysis

The captured images were post-processed using ImageJ for quantification of cell migration and viability. Specifically, for area measurements, the captured images were converted to 8 bit images, after which the threshold was adjusted to convert them into binary images. Areas were calculated based on the limit of the threshold in each image and expressed as a normalized value, $X_{\text{normalized}} = (X - X_{\text{min}}) / (X_{\text{whole area}} - X_{\text{min}})$. The percentage of cell viability was evaluated by the number of live cell / (the number of live cells + dead cells) * 100.

2.6. Statistics

For statistical significant determination of cell migration, we perform a one-way ANOVA test followed by post-hoc Bonferroni correction. Statistical difference is set $p < 0.05$ with significance.

3. Results and Discussion

3.1. Characterization of TPE Bonding

We first studied the bonding strength of the TPE and PDMS materials by measuring the delamination pressures in the microchannel devices. We treated the assembled samples under three different conditions: (1) at room temperature without any heat treatment after device assembly, (2) with heat treatment, after assembly at 37 °C for 2 h and (3) with a heat treatment after assembly at 65 °C for 2 h. Figure 2b shows the delamination pressures of TPE and PDMS on glass slide and PS substrates under those bonding conditions. The resulting data show that the delamination pressures of TPE on the glass slide and PS substrates are about 3.4 and 7 times higher than that of PDMS cases, respectively, without subjecting to any post heat treatment after being assembled at room temperature. When the assembled sample is thermally treated, the bonding strength of the TPE against both the glass slide surface and the PS surface is enhanced with increasing heat treatment temperature, while the bonding strength of PDMS remains relatively unchanged. Furthermore, the bonding strength of TPE against the PS substrate twice as strong as that of TPE on the glass substrate.

We believe this is probably due to the difference interface between these materials. The main component of the TPE film is a polymeric chain of styrene-ethylene-butylene-styrene (SEBS) and the PS is polymeric chain of polystyrene which may contribute to increased Van der Waal's interactions at the interface between SEBS and PS, which are stronger those between SEBS and glass (SiO_2). For cell patterning experiments, we bonded TPE posts to the bottom of PS-based 96-well plates and treat posts in CO_2 incubator at 37°C .

Additionally, we also conducted protein adsorption experiments in both PDMS and TPE-based channels and confirmed that TPE is superior to PDMS in terms of protein adsorption issues (see the Supplementary Materials Figure S1).

3.2. Cell Migration Study

We created patterned cells using TPE posts and study fibroblast cell migration in a 96-well plate. Prior to cell migration studies, human fibroblast cells were patterned in a blank rounded shape using the post. Figure 3 shows typical images of the TPE post and cells surrounding the post area on the 96-well plate. The patterned area with the post was about $0.67\text{ mm}^2 \pm 0.09$ ($n = 8$) and could be simply modified by changing the biopsy punch diameter. After seeding and initial cell culture, the post was gently removed using a tweezer. This process allowed us to make a clearly defined area of cells without undue or harsh damage to the cells. Minimally damaged cells are useful for direct studies on tissue repair and wound healing where a complex biological processes occurs [31].

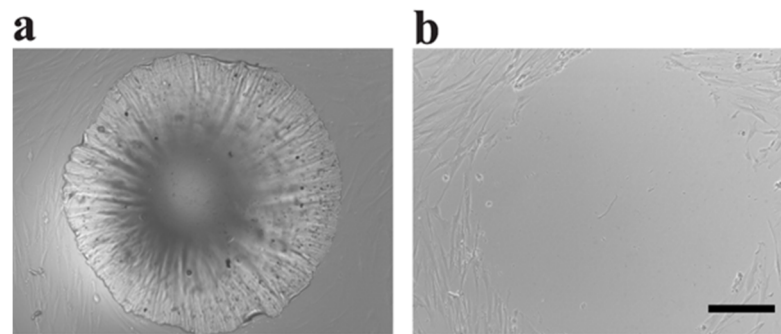


Figure 3. A TPE post and cells. (a) Fibroblasts cells are cultured surrounding the pre-positioned post structure in the 96-well plate. (b) Following post structure removal, the cell migration assay is performed by capturing cell images. The scale bar represents $200\ \mu\text{m}$.

Table 1 lists a comparative study of cell patterning techniques reported in the literature. A comprehensive review of in vitro cell migration assays has been reported by Kramer et al. [32] In this table, we summarize typical cell patterning strategies and compare them with our TPE-based cell patterning method. The uniqueness of our approach lies in the utilization of whole plastic materials, which are highly biocompatible for cell culture and potentially applicable to large-scale and mass manufacturing for cell patterning. In addition, the unique characteristics such as strongly and reversibly bondable on PS make it possible to reuse the devices when multiple chip bonding processes are involved [33].

Table 1. Comparison study of cell patterning techniques.

Technique	Cells	Simplicity	Disadvantages	Advantages
Inkjet printing [34]	Hamster Ovary cells and embryonic motoneurons	Moderate	Low cell viability	High throughput and inexpensive
Scratch assay [2]	Endothelial cells and NIH3T3 cells	Yes	Harshly damaging cells	Relatively easy experimental set-up
Parafilm insert [35]	Retinal epithelial cells and dog kidney epithelial cells	Yes	Limited pattern shapes (circular or striped geometry)	Simple, fast and cheap
Aqueous two-phase cell patterning [4]	HeLa cells and fibroblasts	Moderate	Low throughput	Simple pipette patterning tool
Contact-erasing strategy [36]	Lung adenocarcinoma epithelial cells, 3T3 cells and osteoblast cells	No	Expensive and complicated processes	Multicell micropatterning technique
Tape-assisted microfluidic chip [37]	Cancer cells and fibroblasts	Moderate	Hand-crafted mold type fabrication	Photolithographic-free and cost-effective approach
TPE posts (our approach)	Fibroblasts	Yes	Manual post preparation	High biocompatibility and reversible bonding

Figure 4a shows experimental schematic of the plastic-based cell culture conditions and timeline. The experiment is designed to examine the applicability of our TPE-based cell migration assay after the TPE post removal and also the effect of FBS content in culture media. Figure 4b,c show representative images of the patterned area during cell migration with/without 10% FBS, respectively, using CellTracker and FITC-conjugated phalloidin. In the FBS treated wells, we observed that after 2 days the cells migrated and re-populated the empty area from the prior cell patterning. We also confirmed that the presence of FBS promoted the cell growth and proliferation faster compared to the cells grown without FBS as expected [37,38]. These results suggested that our post-based, cell patterning, assay platform is suitable for cell migration studies and is able to perform quantitative, spatial and temporal analysis of cell culture dynamics. For quantification, we plotted cell migration of the stained cell images by measuring the area “filled-in” of the original patterned region (Figure 5). The resulting graph shows that cells migrated significantly in 24 h in the presence of FBS, while there was no significant difference of in cell migration without FBS.

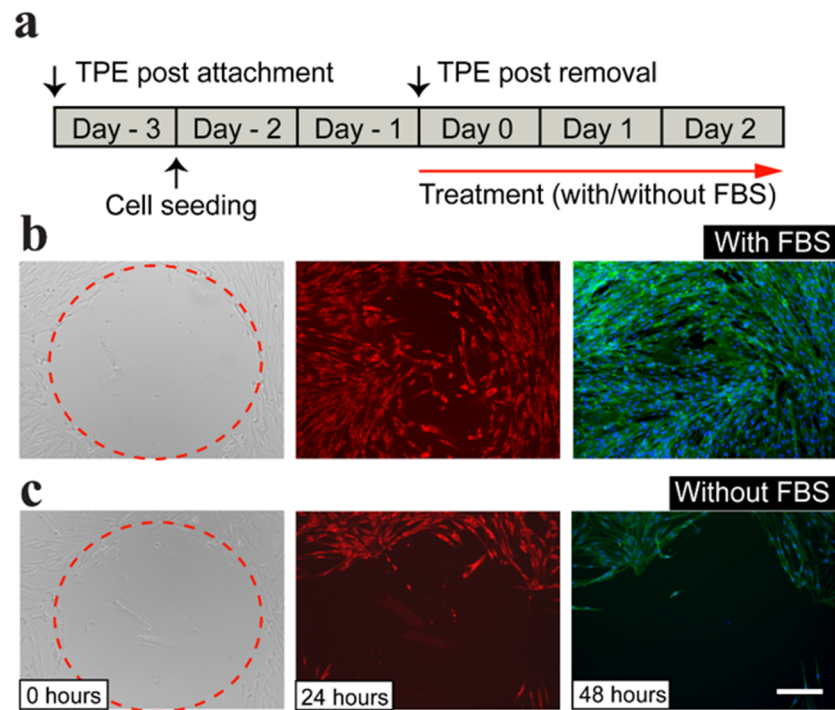


Figure 4. (a) Schematic of the experimental design and timeline of cell treatment. After TPE post removal, cells are cultured for two days in culture media with 10% FBS (b) and without FBS (c). For migration assay, we stain cell using CellTracker (red, 24 h) and phalloidin (green, 48 h). The captured images are post-processed for quantitative analysis. Dashed lines indicates boundary of the original cell patterned area. The scale bar shows 200 μm .

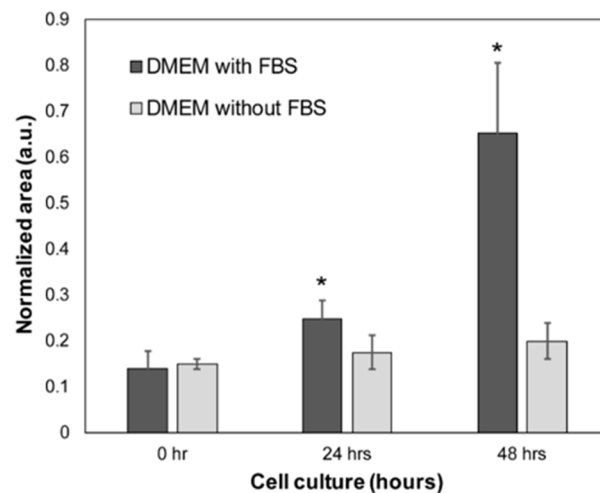


Figure 5. Quantitative analysis of cell migration. The captured images are quantified using ImageJ ($n = 4$). The “filled-in” area is normalized to cell migration. The area covered by cells increases significantly after 24 h with FBS added culture media, arisen from cell migration. Without FBS, there are no significant changes in the measured area.

3.3. Cell Viability Study

We evaluated the cell cytotoxicity of the TPE plug material after it was contacted to the cultured cell in the media. The cells were stained with calcein AM and ethidium homodimer-1 solutions using a LIVE/DEAD assay kit. Figure 6 shows representative images of the stained fibroblast live (Figure 6a) and dead (Figure 6b) cells. We confirmed that most of the fibroblasts and MCF-7 breast cancer cells were alive in 3 day cell culture.

The resulting data showed that the cell viability was over 95% under all conditions. There was no significant difference in cell viability compare to the control group (Figure 6c). The TPE material was therefore highly biocompatible and suitable for cell culture platforms as demonstrated in other cell studies [15].

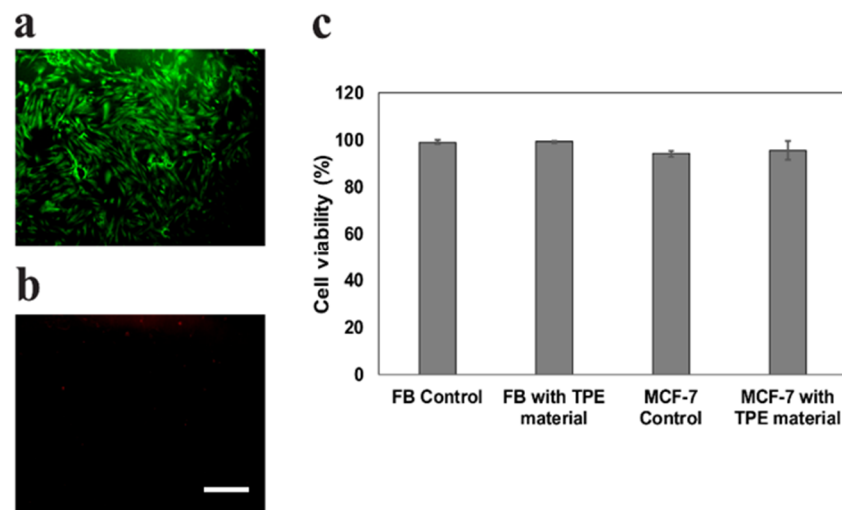


Figure 6. Cell viability test. Representative images of live (a) and dead (b) fibroblasts cell images. The cell cytotoxicity assay is performed using LIVE/DEAD Cell Imaging Kit. (c) A portion of a TPE plug is submerged in cell culture media to examine the release of toxic chemicals from the as-fabricated TPE materials. There is no significant difference of the cell viability for both fibroblasts and breast cancer cells compare to the control groups—no TPE plugs are submerged in culture media. The scale bar represents 500 μm .

4. Conclusions

In this paper, we present reversibly bonded TPE materials used to generate patterns in culture well plates for cell patterning and migration applications. The TPE post feature is bonded to commercially available polystyrene-based culture plates before cell seeding and removed for cell proliferation. This patterning approach induces minimal damage to cells in the defined area and is useful for *in vitro* studies in tissue repair and wound healing.

In cell migration studies, we show the significance of cell growth with FBS-cell culture media compared to the cells cultured without FBS. The cell viability assays also confirm that the TPE material is highly suitable as a culture platform. This is the first example of wholly plastic-based material and fabrication approach, which is appropriate for large-scale and mass manufacturing of cell patterning devices.

In future work, a co-culture patterning platform will be used to culture different cell types by predefining the relative geometrical and spatial configurations of the two interacting cell culture lines. In the technical aspect, upon the photolithography and hot embossing processes, the sub 10 μm patterning on the TPE used in bonding strength test could be also possible to extend the current rounded shape patterning to heterogeneous micropatterning [39].

For future applications, we anticipate this method can be utilized in cell-to-cell communication studies, for example, angiogenesis [40].

Supplementary Materials: The following are available online at <https://www.mdpi.com/2227-9717/9/1/54/s1>. Figure S1: Comparison experiments of protein absorption on the PDMS and TPE channel surfaces. Two identical devices of PDMS and TPE channels were prepared and bonded on the glass slide substrates. The device has two parallel channels as shown (a). We introduced fluorescently-labelled bovine serum albumin (BSA) into the channels with a 1 mg/mL BSA-FITC concentration (a). The devices were then placed in the CO_2 incubator at 37 $^\circ\text{C}$ for 30 min. After washing with PBS, we captured fluorescence images (b) with PDMS channels and (c) TPE channels. The

dashed line represents a plot line of the fluorescent intensity. The scale bar shows 500 μm . (d) The plot graph shows a significant difference of the fluorescent intensities of PDMS and TPE channels. Thus, we confirmed that TPE has less protein adsorption issues than PDMS.

Author Contributions: Initiating project, B.-U.M., K.M. and T.V.; experiments and data analysis, B.-U.M., K.L. and C.M.-G.; draft preparation, B.-U.M. and K.L.; review and editing, K.M. and T.V. All authors have read and agreed to the published version of the manuscript.

Funding: This research received no external funding.

Acknowledgments: This work was supported by National Research Council of Canada.

Conflicts of Interest: The authors declare no conflict of interest.

References

1. Boyden, S. The chemotactic effect of mixtures of antibody and antigen on polymorphonuclear leucocytes. *J. Exp. Med.* **2004**, *115*, 453–466. [[CrossRef](#)] [[PubMed](#)]
2. Liang, C.-C.; Park, A.Y.; Guan, J.-L. In vitro scratch assay: A convenient and inexpensive method for analysis of cell migration in vitro. *Nat. Protoc.* **2007**, *2*, 329–333. [[CrossRef](#)] [[PubMed](#)]
3. Fischer, E.G.; Stingl, A.; Kirkpatrick, C.J. Migration assay for endothelial cells in multiwells. *J. Immunol. Methods* **1990**, *128*, 235–239. [[CrossRef](#)]
4. Frampton, J.P.; White, J.B.; Abraham, A.T.; Takayama, S. Cell Co-culture Patterning Using Aqueous Two-phase Systems. *J. Vis. Exp.* **2013**, *73*, e50304. [[CrossRef](#)]
5. Young, E.W.K. Advances in Microfluidic Cell Culture Systems for Studying Angiogenesis. *J. Lab. Autom.* **2013**, *18*, 427–436. [[CrossRef](#)]
6. Theberge, A.B.; Yu, J.; Young, E.W.K.; Ricke, W.A.; Bushman, W.; Beebe, D.J. Microfluidic Multiculture Assay to Analyze Biomolecular Signaling in Angiogenesis. *Anal. Chem.* **2015**, *87*, 3239–3246. [[CrossRef](#)]
7. Devadas, D.; Moore, T.A.; Walji, N.; Young, E.W.K. A microfluidic mammary gland coculture model using parallel 3D lumens for studying epithelial-endothelial migration in breast cancer. *Biomicrofluidics* **2019**, *13*, 064122. [[CrossRef](#)]
8. Kim, S.; Lee, H.; Chung, M.; Jeon, N.L. Engineering of functional, perfusable 3D microvascular networks on a chip. *Lab Chip* **2013**, *13*, 1489–1500. [[CrossRef](#)]
9. Kang, B.; Shin, J.; Park, H.-J.; Rhyou, C.; Kang, D.; Lee, S.-J.; Yoon, Y.-S.; Cho, S.-W.; Lee, H. High-resolution acoustophoretic 3D cell patterning to construct functional collateral cylindroids for ischemia therapy. *Nat. Commun.* **2018**, *9*, 1–13. [[CrossRef](#)]
10. Toepke, M.W.; Beebe, D.J. PDMS absorption of small molecules and consequences in microfluidic applications. *Lab Chip* **2006**, *6*, 1484–1486. [[CrossRef](#)]
11. Van Midwoud, P.M.; Janse, A.; Merema, M.T.; Groothuis, G.M.M.; Verpoorte, E. Comparison of Biocompatibility and Adsorption Properties of Different Plastics for Advanced Microfluidic Cell and Tissue Culture Models. *Anal. Chem.* **2012**, *84*, 3938–3944. [[CrossRef](#)] [[PubMed](#)]
12. Berthier, E.; Young, E.W.K.; Beebe, D. Engineers are from PDMS-land, Biologists are from Polystyrenia. *Lab Chip* **2012**, *12*, 1224–1237. [[CrossRef](#)] [[PubMed](#)]
13. Moore, T.A.; Brodersen, P.; Young, E.W.K. Multiple Myeloma Cell Drug Responses Differ in Thermoplastic vs PDMS Microfluidic Devices. *Anal. Chem.* **2017**, *89*, 11391–11398. [[CrossRef](#)] [[PubMed](#)]
14. Guillemette, M.D.; Roy, E.; Auger, F.A.; Veres, T. Rapid isothermal substrate microfabrication of a biocompatible thermoplastic elastomer for cellular contact guidance. *Acta Biomater.* **2011**, *7*, 2492–2498. [[CrossRef](#)] [[PubMed](#)]
15. Didar, T.F.; Li, K.; Veres, T.; Tabrizian, M. Separation of rare oligodendrocyte progenitor cells from brain using a high-throughput multilayer thermoplastic-based micro fluidic device. *Biomaterials* **2013**, *34*, 5588–5593. [[CrossRef](#)]
16. Gencturk, E.; Mutlu, S.; Ulgen, K.O. Advances in microfluidic devices made from thermoplastics used in cell biology and analyses. *Biomicrofluidics* **2017**, *11*, 051502. [[CrossRef](#)]
17. Wang, Y.; Chen, H.; He, Q.; Soper, S.A. A high-performance polycarbonate electrophoresis microchip with integrated three-electrode system for end-channel amperometric detection. *Electrophoresis* **2008**, *29*, 1881–1888. [[CrossRef](#)]
18. Tan, H.Y.; Loke, W.K.; Tana, Y.T.; Nguyen, N.-T. A lab-on-a-chip for detection of nerve agent sarin in blood. *Lab Chip* **2008**, *8*, 885–891. [[CrossRef](#)]
19. Kim, M.; Moon, B.-U.; Hidrovo, C.H. Enhancement of the thermo-mechanical properties of PDMS molds for the hot embossing of PMMA microfluidic devices. *J. Micromech. Microeng.* **2013**, *23*, 095024. [[CrossRef](#)]
20. Wan, A.M.D.; Sadri, A.; Young, E.W.K. Liquid phase solvent bonding of plastic microfluidic devices assisted by retention grooves. *Lab Chip* **2015**, *15*, 3785–3792. [[CrossRef](#)]
21. Lu, C.; Lee, L.J.; Juang, Y.J. Packaging of microfluidic chips via interstitial bonding technique. *Electrophoresis* **2008**, *29*, 1407–1414. [[CrossRef](#)]
22. Chen, H.; Wang, L.; Li, P.C.H. Nucleic acid microarrays created in the double-spiral format on a circular microfluidic disk. *Lab Chip* **2008**, *8*, 826–829. [[CrossRef](#)] [[PubMed](#)]

23. Temiz, Y.; Lovchik, R.D.; Kaigala, G.V.; Delamarche, E. Lab-on-a-chip devices: How to close and plug the lab? *Microelectron. Eng.* **2015**, *132*, 156–175. [[CrossRef](#)]
24. Tu, C.; Huang, B.; Zhou, J.; Liang, Y.; Tian, J.; Ji, L.; Liang, X.; Ye, X. A Microfluidic Chip for Cell Patterning Utilizing Paired Microwells and Protein Patterns. *Micromachines* **2016**, *8*, 1. [[CrossRef](#)]
25. Chu, M.; Nguyen, T.T.; Lee, E.K.; Morival, J.L.; Khine, M. Plasma free reversible and irreversible microfluidic bonding. *Lab Chip* **2017**, *17*, 267–273. [[CrossRef](#)] [[PubMed](#)]
26. Geissler, M.; Roy, E.; Diaz-Quijada, G.A.; Galas, J.-C.; Veres, T. Microfluidic Patterning of Miniaturized DNA Arrays on Plastic Substrates. *ACS Appl. Mater. Interfaces* **2009**, *1*, 1387–1395. [[CrossRef](#)]
27. Brassard, D.; Clime, L.; Li, K.; Geissler, M.; Miville-Godin, C.; Roy, E.; Veres, T. 3D thermoplastic elastomer microfluidic devices for biological probe immobilization. *Lab Chip* **2011**, *11*, 4099–4107. [[CrossRef](#)]
28. Li, K.; Morton, K.; Shiu, M.; Turcotte, K.; Lukic, L.; Veilleux, G.; Poncet, L.; Veres, T. Normally Closed Microfluidic Valves with Microstructured Valve Seats: A Strategy for Industrial Manufacturing of Thermoplastic Microfluidics with Microvalves. In Proceedings of the IEEE 33rd International Conference on Micro Electro Mechanical Systems (MEMS), Vancouver, BC, Canada, 18–22 January 2020; pp. 1110–1113.
29. Li, K.; Hernandez-Castro, J.A.; Turcotte, K.; Morton, K.; Veres, T. Superhydrophobic Thermoplastic Surfaces with Hierarchical Micro-Nanostructures Fabricated by Hot-Embossing. In Proceedings of the IEEE 20th International Conference on Nanotechnology (IEEE-NANO), Montreal, QC, Canada, 29–31 July 2020; pp. 81–84.
30. Clime, L.; Li, K.; Geissler, M.; Hoa, X.D.; Robideau, G.P.; Bilodeau, G.J.; Veres, T. Separation and concentration of *Phytophthora ramorum* sporangia by inertial focusing in curving microfluidic flows. *Microfluid. Nanofluid.* **2016**, *21*, 5. [[CrossRef](#)]
31. Eming, S.A.; Martin, P.; Tomic-Canic, M. Wound repair and regeneration: Mechanisms, signaling, and translation. *Sci. Transl. Med.* **2014**, *6*, 1–36. [[CrossRef](#)]
32. Kramer, N.; Walzl, A.; Unger, C.; Rosner, M.; Krupitza, G.; Hengstschläger, M.; Dolznig, H. In vitro cell migration and invasion assays. *Mutat. Res.* **2013**, *752*, 10–24. [[CrossRef](#)]
33. Wan, A.M.D.; Devadas, D.; Young, E.W.K. Recycled polymethylmethacrylate (PMMA) microfluidic devices. *Sensors Actuators B Chem.* **2017**, *253*, 738–744. [[CrossRef](#)]
34. Xu, T.; Jin, J.; Gregory, C.; Hickman, J.J.; Boland, T. Inkjet printing of viable mammalian cells. *Biomaterials* **2005**, *26*, 93–99. [[CrossRef](#)] [[PubMed](#)]
35. Javaherian, S.; O'Donnell, K.A.; McGuigan, A.P. A fast and accessible methodology for micro-patterning cells on standard culture substrates using parafilmTM inserts. *PLoS ONE* **2011**, *6*, e20909. [[CrossRef](#)] [[PubMed](#)]
36. Li, Y.; Jiang, X.; Zhong, H.; Dai, W.; Zhou, J.; Wu, H. Hierarchical Patterning of Cells with a Microeraser and Electrospun Nanofibers. *Small* **2015**, *12*, 1230–1239. [[CrossRef](#)] [[PubMed](#)]
37. Zhao, L.; Guo, T.; Wang, L.; Liu, Y.; Chen, G.; Zhou, H.; Zhang, M. Tape-Assisted Photolithographic-Free Microfluidic Chip Cell Patterning for Tumor Metastasis Study. *Anal. Chem.* **2017**, *90*, 777–784. [[CrossRef](#)] [[PubMed](#)]
38. Fang, C.; Wu, C.; Fang, C.; Chen, W. Long-term growth comparison studies of FBS and FBS alternatives in six head and neck cell lines. *PLoS ONE* **2017**, *12*, e0178960. [[CrossRef](#)]
39. Au, H.T.H.; Cui, B.; Chu, Z.E.; Veres, T.; Radisic, M. Cell culture chips for simultaneous application of topographical and electrical cues enhance phenotype of cardiomyocytes. *Lab Chip* **2009**, *9*, 564–575.
40. Nishida, N.; Yano, H.; Nishida, T.; Kamura, T.; Kojiro, M. Angiogenesis in cancer. *Vasc. Health Risk Manag.* **2006**, *2*, 213–219. [[CrossRef](#)]